E-proceedings of the 36th IAHR World Congress,
28 June – 3 July, 2015, The Hague, the Netherlands

LABORATORY STUDY OF GRADUALLY-VARIED FLOW THROUGH SUBMERGED SEMI-RIGID BLADE-TYPE VEGETATION

BUSARI, AFIS OLUMIDE[1] & LI, CHI WAI[2]

[1] Department of Civil and Environmental Engineering, The Hong Kong Polytechnic University, Hong Kong SAR, China, e-mail: mscbusari@gmail.com

[2] Department of Civil and Environmental Engineering, The Hong Kong Polytechnic University, Hong Kong SAR, China, e-mail: cecwli@polyu.edu.hk

ABSTRACT

The condition of flow through a vegetation patch is gradually-varied. The drag generated by vegetation depends on the shape of each piece of vegetation and the flow interaction among the vegetation elements. Some vegetation is of blade-type which has different drag characteristics as compared to the circular-cylinder type vegetation. In the present study experiments are carried out to investigate the hydrodynamic behavior of gradually-varied flow through blade-type vegetation. Particular attention is focused on the effect of distribution pattern of vegetation elements on the total drag generated by a vegetation patch. The values of the density parameter of vegetation ($\lambda = Nb_v$, N is areal density, b_v is the blade width) are 72, 48, 24, 18, 15, 12, 6 and 3 (1/m). The blade Reynolds number Re using the blade width as the length scale ranges from 670 to 1110 and six flow rates are used in each set of experiments. Theoretical longitudinal momentum equation relating the vegetation resistant force, water surface slope and mean velocity in the vegetation layer is used to determine the averaged drag coefficient C_d. Using a regular-array pattern of vegetation elements, the sheltering effect and channeling effect are studied separately by varying the longitudinal element spacing (S_y) and lateral element spacing (S_x) respectively. For a constant lateral element spacing (S_x), C_d decreases with increasing areal density of vegetation due to sheltering effect. For a constant longitudinal spacing (S_y), C_d increases with increasing areal density of vegetation due to channeling effect. The results show that apart from the density parameter λ, the distribution pattern of vegetation elements can exert significant effect on the drag coefficient and the associated flow characteristics.

Keywords: Drag coefficient, interference mechanisms, submerged vegetation, semi-rigid blade.

1. INTRODUCTION

The hydrodynamics of vegetated flows in open channels, rivers and streams is complicated due to the wide variation in the flow conditions and vegetation characteristics. Submerged, emergent or floating vegetation will lead to different flow behaviors. Also the variation in shape, size, structure, distribution pattern and stage of growth of vegetation elements will affect the flows. The study of flow through emergent circular-cylinder type vegetation is well documented (e.g., Nehal et al., 2012; Cheng and Nguyen, 2011; Tanino and Nepf, 2008; Stone and Shen, 2002). The more complicated case of flow over submerged vegetation has also been investigated (Nepf, 2012; Zong and Nepf, 2010; Stoesser et al., 2010; Kothyari et al., 2009; White and Nepf, 2007; Ishiwaka et al., 2000; Wu et al., 1999 and Nepf, 1999). The governing equation for steady flow through vegetation describes the balance of drag force and the flow momentum absorbed by vegetation elements. In case of gradually-varied flow through emergent vegetation, the pressure forces and hence the water surface gradient need to be included in the governing equation. The drag coefficient can be determined by a numerical integration procedure (Busari and Li, 2015; Li and Tam, 2002). For flows over submerged vegetation, the determination of flow resistance is more complicated. The resistance force is dependent on the flexibility, frontal projected area and submergence ratio of vegetation (Jarvela, 2004; Stone and Shen, 2002; Jarvela, 2002). More information on the vegetation properties thus is required.

In the determination of vegetation induced hydraulic resistance in open channel flows using theoretical models, semi-empirical models or numerical models (e.g. Busari and Li, 2014; Jarvela, 2004; Fathi-Moghadam and Kouwen, 1997), the key parameter needed to be specified is the drag coefficient C_d of the vegetation stems. For rigid vegetation, the Rigid Cylinder Analogy (RCA) is commonly used (e.g., Baptist et al., 2007; Huthoff et al., 2007) in which the vegetation stems are treated as rigid cylinders. The flow is then affected by the wake interference among the cylinders (Schoneboom et al., 2011). Aberle and Jarvela, (2013) pointed out the the RCA is not adequate enough for real plants, and the geometric and stiffness properties of vegetation are required for more accurate determination of the drag coefficient.

In this study, focus is on the vegetation with high areal density and low submergence ratio ($h/k<1.6$, h is the water depth and k is the vegetation height). The areal density of vegetation gives a resistance parameter $\eta=\lambda k$ ($\lambda=Nb_v$, $N(1/m^2)$ is number of stems per unit horizontal area; $b_v(m)$ is width of stem) which is greater than the threshold value for the generation of canopy scale turbulence defined in Nepf (2012) and falls in the dense canopy range $\eta \geq 0.23$. The bed shear force is negligible as compared to the vegetation induced drag. The main objective of this paper is to study the interference mechanisms (channeling and sheltering) among vegetation stems under a gradually-varied flow condition. Regular arrays of blade-type vegetation stems are employed and each interference mechanism is studied independently

by using appropriate array patterns. The effects of areal density of vegetation on the drag coefficient, vertical profiles of streamwise mean velocity and vertical distribution of Reynolds stress are investigated.

2. LABORATORY EXPERIMENTS

The laboratory experiments were conducted in a 0.31 m wide, 0.40 m deep and 12.50 m long tilting and slope–adjustable rectangular flume. The sidewalls and bottom of the channel are made of glass and steel respectively. Flow rates were measured by an electromagnetic flowmeter installed in the flow return pipe. The flow at the entrance of the channel was straightened using honeycomb grids, thereby preventing the formation of large-scale flow disturbances. The flume received a constant supply of water from a head tank. An adjustable tailgate was installed at the downstream end of the flume to regulate the flow depth. Water leaving the flume entered a large sump under the flume, where it was recirculated to the constant head tank by a pump. Two wheeled trolleys, which can be moved along the double-rail track on the top of the flume, were used to mount the Vernier point gauge. The channel surface slope was calculated from the longitudinal flow-depth variation, which was measured with the point gauge with $\pm$1 mm accuracy.

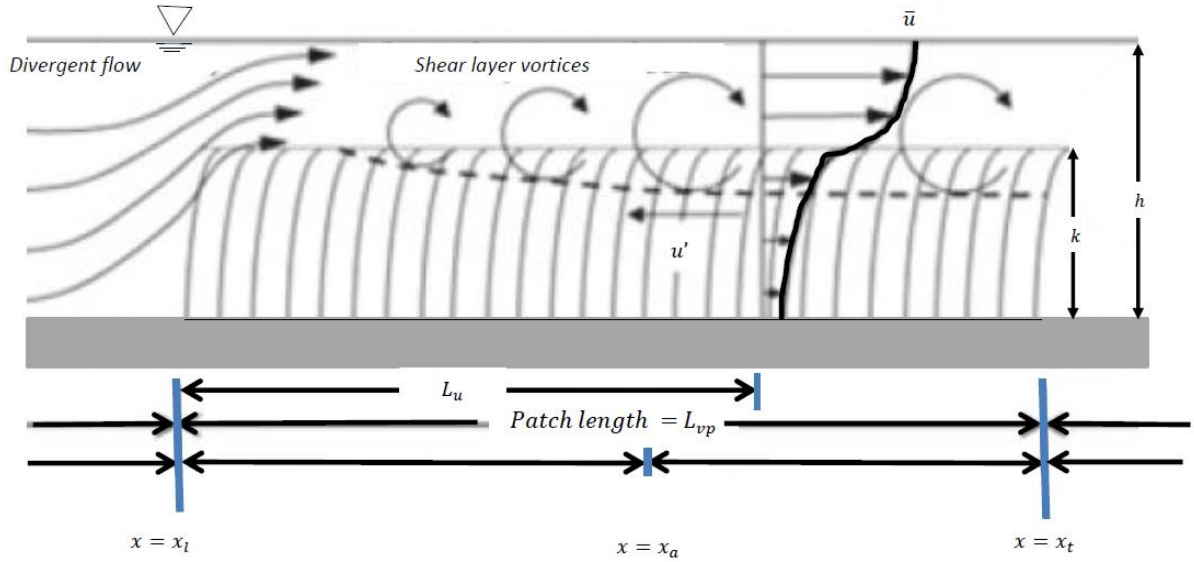

Figure 1: Schematic diagram of the longitudinal section of the flume

Figure 1 shows the schematic diagram of the longitudinal section of the flume. The longitudinal direction is represented as x, with subscripts l, a and t denoting the locations of leading edge, adjustment region and trailing edge respectively. A preliminary investigation of the fully developed region was carried out by measuring the vertical profiles of velocity longitudinally. The result suggested that the fully developed region can be estimated using the empirical equation proposed by Zeng and Li (2014) for the adjustment length of the transitional region of the vegetation patch.

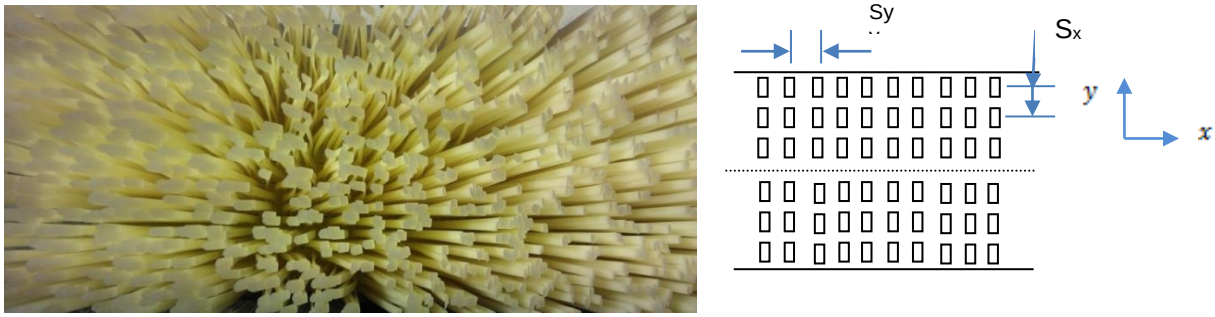

Figure 2: A sectional plan view of the dense vegetation (ϕ =0.121 arrays)

The vegetation patch is of length of 2.4m long and 0.3 m wide, and was formed with an array of semi-rigid cable tile blades. The blades are of 250mm height, 7.53mm width and 1.68mm thickness, and fixed on a PVC board placed at the

bed of the channel. The fixing pattern of the blades is regular with the longitudinal spacing denoted by S_y(m) and lateral spacing denoted by S_x(m) (Figure 2). The spacing of blade elements is different for different boards which were placed on the channel bed alternatively. The fraction of horizontal area occupied by vegetation is given by $\phi = Nb_V t_V$ (-), b_v (m) and t_v (m) are width and thickness of the blade. The vegetation density parameter is defined by $\lambda = \frac{b_v}{S_x S_y} = Nb_v$ (m^{-1}). In the experiments the vegetation density λ(m^{-1}) ranges from 3 to 72.

The velocity measurements were carried out using a 3D side-looking Acoustic Doppler Velocimeter (ADV) Vectrino (NORTEK). Due to the high areal density of the vegetation patch, some blades were removed near the trailing edge for velocity measurements, after water level measurements were completed. To capture the turbulence fluctuations, the sampling rate of 75Hz was employed for most experiments except that for cases with λ = 72 and 48, the sampling rate was set to 200 Hz and 150 Hz respectively. Sampling record of 120 s duration was taken at each point to provide reliable estimation of the mean and turbulence quantities. To increase the accuracy and reliability of the measurements, the signal-noise ratio (SNR) and the correlation (COR) parameters were evaluated (Zeng, 2011; Wahl, 2000). The raw data were processed if the COR is greater than 70% threshold and the SNR is greater than 5dB. Based on these criteria, more than 75% of the samples were retained in the time series.

Table 1 summarizes the key hydraulic parameters of the experiments. The discharge was varied between 25 m^3/hr and 50 m^3/hr at the interval of 5m^3/hr. The locations of the vertical velocity measurements were identical for all experiments because the location is far beyond the adjustment length obtained through observations and the empirical equation proposed in Zeng and Li, (2014). The velocity was measured at 10mm interval along the vertical and in some cases at 5mm in the clear water region (i.e., above vegetation layer). The number of velocity measurement along the vertical is not less than 25 for all cases. The longitudinal water depth profile was measured at the middle of the channel using the Vernier point gauge at 5cm interval for cases with S_x=0.0125m and at 10cm interval for cases with S_y=0.025m.

The flow is spatially varied due to the finite vegetation patch length. Increasing the discharge leads to the increases in water level, as well as the velocity, particularly in the clear water region. The side looking ADV measures velocity at locations at least 2cm below the water surface. The measured velocity profile cannot give the actual mean velocity since the velocity is not uniform across the channel. To estimate the portion of flow within the vegetation region, the following approach is used.

$$Q_v = \left(\frac{Q_1}{Q_1 + Q_2}\right) \times Q_{in} \quad ; \qquad Q_a = \left(\frac{Q_2}{Q_1 + Q_2}\right) \times Q_{in} \tag{1}$$

where Q_v is the flow rate in the vegetation region, Q_a is the flow rate in the clear water region, Q_{in} is the total flow rate in the open channel and, Q_1 and Q_2 are given by $Q_1 = B\int_{z=0}^{z=k} udz$ and $Q_2 = B\int_{z=k}^{z=h} udz$ respectively, B is the channel width and z is the vertical ordinate. Experiments shown that the increase in the total flow rate Q_{in} mainly increases the flow rate in the clear water zone, whereas the flow rate within the vegetation zone is almost constant.

It was observed that the simulated plants were deflected (most significantly at the leading edge) and swayed during the experiments (Figure 3). The deflection is however small due to the high flexural rigidity of vegetation. Generally, the deflected height exceeded 99.2% of the original height.

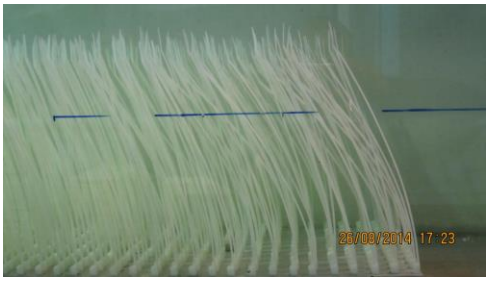

Figure 3: Swaying plants

Table 1: Key parameters of the experiments

Placement patterns of vegetation elements (*m*)	Q (m^3/s)	h (*m*)	U (*m/s*)	Re (-)	λ (m^{-1})
		S_x = constant			
	0.00694	0.2830	0.0901	678	
	0.00833	0.3110	0.0984	740	
S_X = 0.0125	0.00972	0.3300	0.1082	815	72.29
S_Y = 0.0083	0.01111	0.3400	0.1120	904	
	0.0125	0.3565	0.1287	969	
S_X = 0.0125	0.00833	0.2868	0.1020	768	
S_Y = 0.0125	0.00972	0.2963	0.1152	867	48.19
	0.01111	0.3043	0.1282	965	
	0.0125	0.3120	0.1406	1059	
	0.01388	0.3190	0.1528	1151	
S_X = 0.0125	0.00833	0.2865	0.0978	736	24.10
S_Y = 0.0250	0.00972	0.2970	0.1100	829	
	0.01111	0.3040	0.1228	925	
	0.0125	0.3112	0.1350	1016	
	0.01388	0.3178	0.1469	1106	
S_X = 0.0125	0.00833	0.2830	0.0969	730	
S_Y = 0.0500	0.00972	0.2950	0.1085	817	12.05
	0.01111	0.3020	0.1209	911	
	0.0125	0.3110	0.1321	995	
	0.01388	0.3175	0.1440	1085	
S_X = 0.0125	0.00833	0.2810	0.0960	723	6.024
S_Y = 0.100	0.00972	0.2935	0.1079	813	
	0.01111	0.3010	0.1203	906	
	0.0125	0.3090	0.1318	992	
	0.01388	0.3145	0.1439	1084	
		S_y = constant			
	0.00833	0.2835	0.0956	717	6.024
S_X = 0.050	0.00972	0.2935	0.1080	809	
S_Y = 0.0250	0.01111	0.3010	0.1203	901	
	0.0125	0.3085	0.1320	989	
	0.01388	0.3160	0.1432	1073	
					3.012
	0.00833	0.2820	0.0958	721	
S_X = 0.100	0.00972	0.2915	0.1082	814	
S_Y = 0.0250	0.01111	0.2970	0.1213	913	
	0.01250	0.3040	0.1333	1003	
	0.01388	0.3105	0.1450	1092	

3. THEORETICAL FORMULATIONS

In unidirectional flow over vegetation, the channel cross-sectional averaged velocity U is given by

$$U = Q \Big/ Bh\left(1-\phi\frac{k}{h}\right) \tag{2}$$

where Q (m^3/s) is the flow rate; B (m) is the channel width. The total drag force F_d (N) due to pressure differences on the plant surfaces in a unit volume can be defined by

$$F_d = 0.5\lambda C_d \rho k U^2 \tag{3}$$

where; C_d (-) is the drag coefficient, ρ(kg/m^3) is the density of water. The shear force on plant surfaces due to viscous stresses is assumed small and is accounted in the expression of F_d.

In the analysis it is assumed that the only source of energy dissipation is due to current-vegetation interaction. For an open channel flow through vegetation, over a small longitudinal distance, Δx , a change in the hydraulic head (water level difference), Δz is resulted. By applying the principle of conservation of momentum, the one-dimensional momentum balance equation is as follows.

$$\left(\lambda C_d k \frac{Q^2}{2Bh^2\left(1-\phi\frac{k}{h}\right)^4} - gBhS \right) = -\left(gBh - \frac{Q^2}{Bh^2} \right)\frac{\Delta z}{\Delta x} \qquad (4)$$

where g (m/s^2) is the gravitational acceleration and S is the channel bottom slope. The first to fourth term of equation (4) represents the drag force, body force, pressure force and the rate of change of momentum flow rate respectively. The value of C_d can be evaluated from equation (4) by measuring the flow rate and water surface profile.

4. RESULTS AND DISCUSSIONS

4.1 Adjustment length and velocity profiles in clear water zone

To determine the adjustment length L_u beyond which uniform flow condition is reached, profiles of the longitudinal velocity about the clear water region at different vertical transects along the longitudinal center-line were measured using an ADV. Figure (4) shows the velocity profiles for the case of vegetation with high areal density (λ = 48) at z = 4.8, 5.05 and 5.2m, corresponding to 2.0, 1.75 and 1.6m downstream of the leading edge of the vegetation edge. Convergence of the profiles is observed and it is expected that the convergence of the velocity profiles within the vegetation zone should also be reached. Consequently, velocity measurements were conducted for the whole vertical transect at 2.2m downstream of the leading edge. Blades were removed to enable the velocity measurements within the vegetation zone.

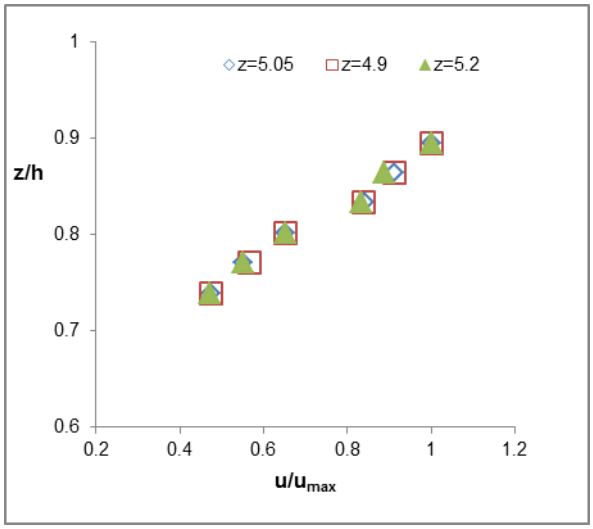

Figure 4: Streamwise mean velocity profiles in clear water zone

Further confirmation that the uniform flow condition is reached at 2.2m downstream of the leading edge is done by using the empirical equation proposed by Zeng and Li (2014) for mean velocity.

$$L_u = 1.5\frac{U_m}{\sqrt{-(u'w')_{max}}} \qquad (5)$$

where U_m is the mean velocity, $-(u'w')_{max}$ is the peak Reynolds stress per unit mass. Based on the velocity measurements for cases of vegetation with different areal densities and different flow rates, the empirical equation (5)

yields $0.48m \leq L_u \leq 0.83m$ for 6 $m^{-1} \leq \lambda \leq 72$ m^{-1}. The adjustment length is found to increase with increasing flow rate and decrease with increasing areal density of vegetation.

4.2 Flow and drag characteristics

Figure 5 shows the velocity profile and distribution of turbulence stresses for cases with different values of vegetation density λ and constant lateral spacing (S_x=0.0125m). For every distribution pattern of blades six sets of experiments of different flow rates (Table 1) were conducted. Here only the results for Q = 0.0125m^3/s is reported as other sets of results are of similar trends. Figure 5a shows that the velocity profile within the vegetation zone is approximately uniform for all cases. The apparent effect is the increase of water level for increasing flow rate. For a given flow rate, the longitudinal velocity in the vegetation zone increases with decreasing vegetation density λ (Figure 5a). The distribution of the velocity in the clear water zone is affected by turbulence penetration. The velocity profile in the clear water zone can be described by an exponential function. A sharp change in the velocity gradient occurs at the interface between vegetation zone and clear water zone for all cases. This implies that the shear force on plant surfaces due to viscous stresses can be significant. Since the vegetation height is close to the water depth, intensive turbulence exchange occurs in the clear water zone. The Reynolds stress increases with vegetation density λ and turbulence penetration increases with decreasing λ (Figure 5b).

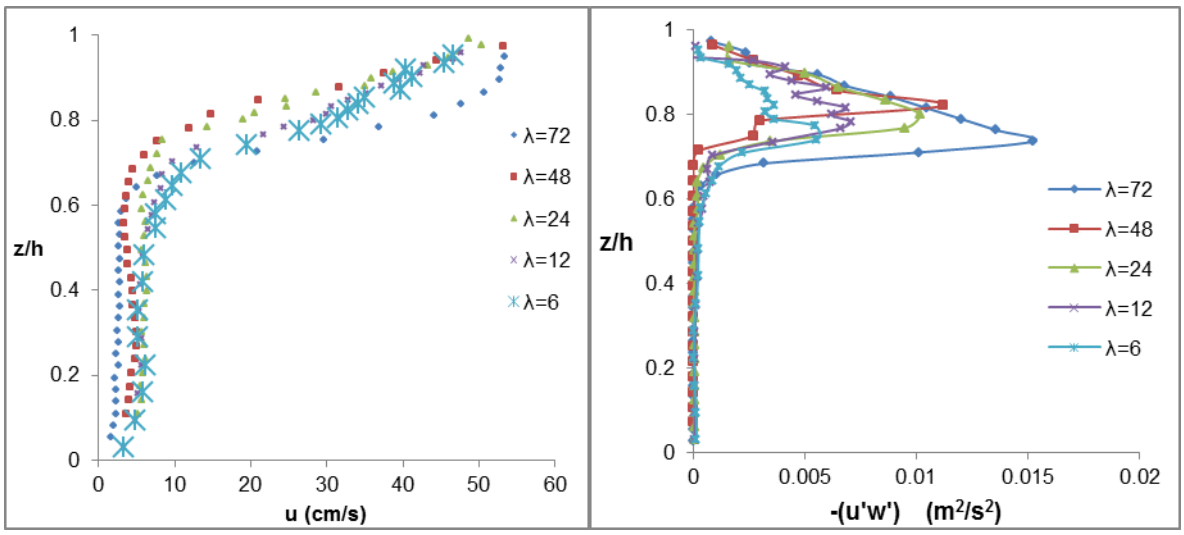

Figure 5: Cases with S_x=0.0125m. (a) vertical mean velocity profiles and (b) vertical distribution of Reynolds stress

As shown in figure (6a), the drag coefficient decreases with increasing Reynolds number. the relationship is best described with exponential law as follows:

$$\left.\begin{aligned} C_d &= ae^{b\,\mathrm{Re}} \\ a &= f(\phi) \end{aligned}\right\}$$

Where a is a parameter that decreases with increasing vegetation density λ (with S_x = constant) and b is a constant (= 0.002). The correlation coefficient of the fitting is very high, greater than 0.99.

Figure (6b) illustrates that higher areal density of vegetation causes the decrease of drag coefficient due to sheltering effect among vegetation stems. The drag coefficient is dependent on the flow rate at low vegetation density λ. Large flow rate causes a smaller value of C_d. The effect of increasing flow rate is less significant at higher densities since the blades behave as a continuum. In Figure (6c), the resistance force defined as a function of U_v (which is the mean velocity in the vegetation zone) is almost asymptotic at higher densities. This is because large portion of the flow is diverged over the blades due to the closeness between the blades. Therefore, the flow in vegetation layer is low and eddies are weak in the gaps and wake formation is strongly interfered. As S_x increases, the intrusion of flow into gaps becomes stronger and C_d increases as flow within the blades increases. By using the mean velocity described in eqn. 2 to define resistance force (see Figure 6d), a clear trend similar to that observed in (Figure 6b) is seen and the discrepancy due to increasing flow rates at lower densities reduces.

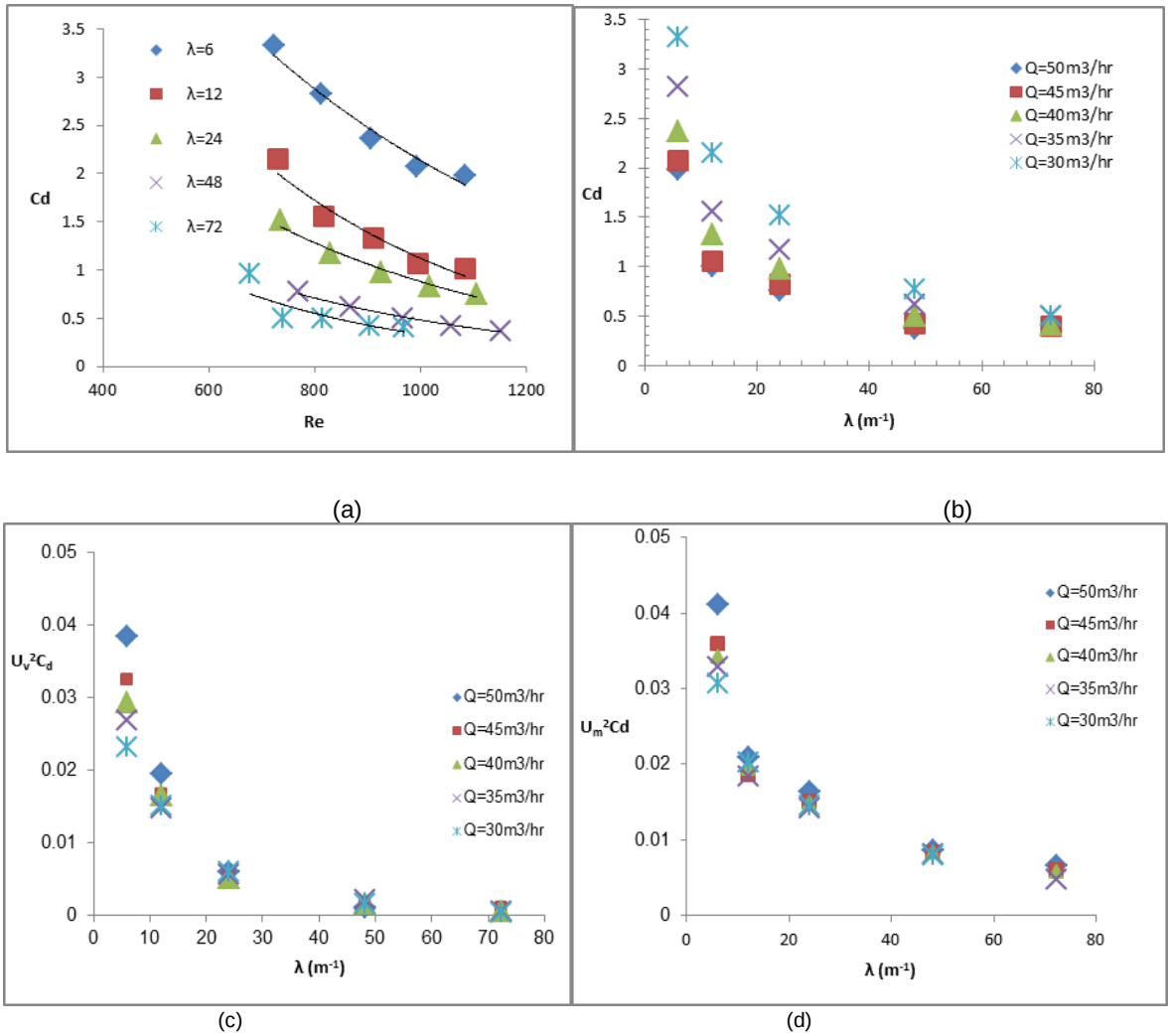

Figure 6: Effect of vegetation density on resistance force and drag coefficient
(U_v = mean velocity in the vegetation zone and U_m= mean velocity described by eqn.2)

4.3 Effect of vegetation distribution pattern

The effect of vegetation distribution pattern on the flow characteristics is investigated by using two cases of experiments. The first case is of S_x=0.0125m, S_y=0.1m, and the second case is of S_x=0.05m, S_y=0.025m. Both cases have the λ value of 6 m^{-1}. Figure 7 shows the velocity profiles and Reynolds stress profiles for the discharge of 0.0125m^3/s. In Figure 7a, the difference of the mean velocity in the vegetation zone and that in the clear water zone is lesser for the case with S_x=0.05m. Thus more water flows over the vegetation for the case with S_x=0.0125m, indicating that the resistance in the vegetation zone is higher. This is confirmed by the higher peak Reynolds stress measured (Figure 7b). Physically the case with S_x=0.0125m has a narrower lateral stem spacing which allows lesser flow to pass through the vegetation zone.

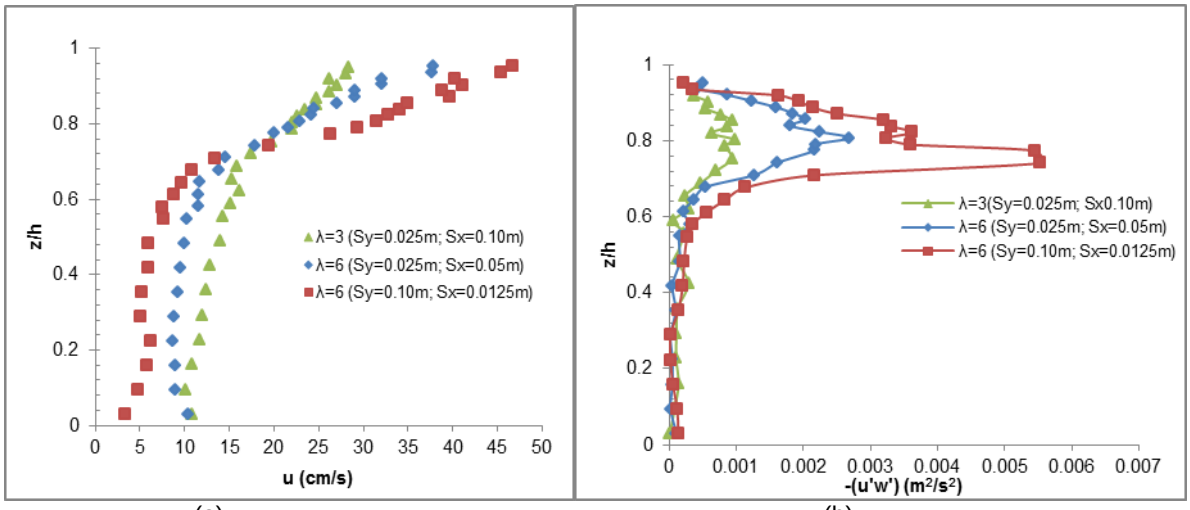

(a) (b)

Figure 7: (a) vertical mean velocity profiles and (b) vertical distribution of Reynolds stress for λ=3m^{-1} and 6m^{-1}.

The effect of increasing the lateral spacing is investigated by adding the case with S_x=0.01m and S_y=0.025m, with λ=3m^{-1}. Comparing to the case with Sx=0.05m, Sy=0.025m (λ=6m^{-1}), the case with λ=3m^{-1} allows more water pass through the vegetation zone. The flow resistance is smaller and thus the peak Reynolds stress and the drag coefficient is lower (Figure 8). This two sets of results show that the drag coefficient increases with the vegetation density λ, which is of the opposite trend with that shown in Figure 6b. By fixing the value of S_y for the two cases, the sheltering effect remains more or less constant. Increasing S_x allows more water flowing through the vegetation zone and reduces the hydraulic resistance. The effect is referred as the channeling effect.

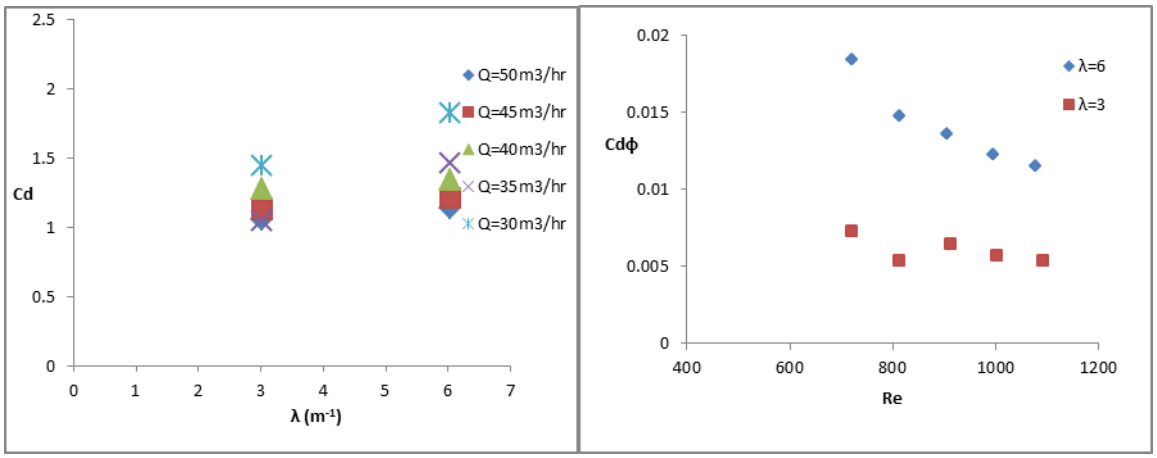

(a) (b)

Figure 8: Effect of vegetation density on drag coefficient (S_y=0.025m)

5. CONCLUSIONS

The characteristics of gradually-varied flows through semi-rigid blade-type vegetation have been investigated experimentally. The areal density of vegetation is high and ranges from λ=3m^{-1} to 72m^{-1}. Two interference mechanisms among the vegetation stems are identified: sheltering and channeling. For regular arrays of blades with constant lateral stem spacing (S_x), the drag coefficient C_d decreases with increasing areal density of vegetation due to sheltering effect. For arrays of blades of constant longitudinal spacing (S_y), C_d increases with increasing areal density of vegetation due to channeling effect. The results show that apart from the density parameter λ, the distribution pattern of vegetation elements can affect significantly the drag coefficient and the associated flow characteristics, including flow adjustment length, peak Reynolds stress and flow division in the clear water zone and vegetation zone.

ACKNOWLEDGEMENT

This work is supported by the Research Grant Council of the Hong Kong Special Administrative Region under Grant No. 5200/12E and a grant from the Hong Kong Polytechnic University.

REFERENCES

Aberle, J and Jarvela, J., (2013). *Flow resistance of unsubmerged rigid and flexible floodplain vegetation*. Journal of Hydraulic research, Volume 51, number 1, pp 33 – 45.

Busari, A.O and Li, C.W., (2014). *A hydraulic roughness model for submerged flexible vegetation with uncertainty estimation*. Journal of Hydro-environment Research.

Busari, A.O and Li, C.W., (2015). *A laboratory study of gradually varied flow through semi-rigid unsubmerged blade-type vegetation*. Proceedings of EMI (ASCE) International conference, Hong Kong.

Baptist, M.J, Babovic, V, Keijzer, M, Uttenbogaard, R.E, Mynett, A and Verwey, A., (2007). *On inducing equations for vegetation resistance*. Journal of Hydraulic Research, Volume 45, Number 4, pp 435 -450.

Cheng, N.S and Nguyen, H.T., (2011). *Hydraulic radius for evaluating resistance induced by simulated unsubmerged vegetation in open-channel flows*. Journal of Hydraulic Engineering, Volume 137, number 9, pp 995 -1004.

Fathi-Moghadam, M., Kouwen, N. (1997). *Nonrigid, nonsubmerged vegetative roughness on floodplains*. Journal of Hydraulic Engineering, volume 123, issue 1, pp 51–57.

Jarvela J., (2002). *Flow resistance of flexible and stiff vegetation: a flume study with natural vegetation*. Journal of Hydrology, volume 269, pp 44–54

Jarvela J., (2004). *Determination of flow resistance caused by non-submerged woody vegetation*. International of Journal of River Basin Management. Volume 2, number 1, pp 61–70.

Huthoff, F., Augustijn, D and Hulscher, S., (2007) *Analytical solution of the depth-averaged flow velocity in case of submerged rigid cylindrical vegetation.* Water Resources Research 43:W06413. doi:10.1029/2006WR005625

Ishikawa, Y., Mizuhara, K., and Ashida, S. (2000). *Effect of density of trees on drag exerted on trees in river channels*. Eurasian Journal of Forest Research, Volume 5, number 4, pp 271–279.

Kothyari, U. C., Hayashi, K., and Hashimoto, H., (2009). *Drag coefficient of unsubmerged rigid vegetation stems in open channel flows*. Journal of Hydraulic Research, Volume 47, number 6, pp 691 – 699.

Li, C.W and Tam, Y.F., (2002). *Gradually varied flow through semi-rigid vegetation*. The proceedings of the 14th Congress of International Association of Hydraulic Engineering and Research (IAHR), Hong Kong, 15-18 December, 2004, pp 859-864.

Nehal, L., Yan, Z.M., Xia, J.H and Khaldi, A., (2012*). Flow through non-submerged vegetation: A flume experiment with artificial vegetation*. 16th International Water Technology conference, IWTC, Istanbul, Turkey.

Nepf, H.M. (1999). *Drag, turbulence, and diffusion in flow through unsubmerged vegetation*. Journal of Water Resources. Volume 35, number 2, pp 479–489.

Nepf, H.M. (2012). *Hydrodynamics of vegetated channels*. Journal of Hydraulic Research, volume 50, number 3, pp 262 – 279.

Schoneboom, T., Aberle, J and Dittrich, A., (2011). *Spatial Variability, Mean Drag Forces, and Drag coefficients in an array of rigid cylinders*. Experimental Methods in Hydraulic Research. P. Rowinski (ed.), Geoplanet: Earth and Planetary Sciences, DOI 10.1007/978-3-642-17475-9_18, © Springer-Verlag, Berlin, Heidelberg.

Stoesser, T., Kim, S. J., and Diplas, P., (2010). *Turbulent flow through idealized unsubmerged vegetation*. Journal of Hydraulic Engineering, Volume 136, number12, pp 1003–1017.

Stone, B.M., Shen, H.T., (2002). *Hydraulic resistance of flow in channels with cylindrical roughness*. Journal of Hydraulic Engineering, Volume 128, number 5, pp 500 – 506.

Tanino, Y. & Nepf, H., (2008). *Laboratory investigation of mean drag in a random array of rigid, unsubmerged cylinders*. Journal of Hydraulic Engineering, 134 (1), pp. 34–41.

Wahl, T.L., (2000). *Analyzing ADV data using WinADV*. Proceedings of Joint Conference on Water Resources Engineering and Water Resources Planning and Management. July 30-august, 2000, Minneapolis, Minnesota

White, B and Nepf, H., (2007). *Shear instability and coherent structures in a flow adjacent to a porous layer*. Journal of Fluid Mechanics, volume 593, pp 1 - 32.

Wu, F.C., Shen, H.W., and Chou, Y.J., (1999). *Variation of roughness coefficients for unsubmerged and submerged vegetation*. Journal of Hydraulic Engineering, Volume 125, number 9, pp 934 – 942.

Zeng, C., (2011). *Numerical and experimental studies of flows in open channels with gravel and vegetation roughnesses*. PhD thesis, Department of Civil and Environmental Engineering, The Hong Kong Polytechnic University. 197pp.

Zeng, C and Li, C.W., (2014). *Measurements and modeling of open-channel flows with finite semi-rigid vegetation patches*. Journal of Environmental Fluid Mechanics. Volume 14, pp 113 – 134.

Zong, L and Nepf, H., (2010). *Flow and deposition in and around a finite patch of vegetation*. Journal of Geomorphology, volume 116, pp 363 – 372.

.